Regioselective Bromination and Functionalization of Dibenzo[hi,st]ovalene as Highly Luminescent Nanographene with Zigzag Edges

Qiang Chen, Di Wang, Martin Baumgarten, Dieter Schollmeyer,[b] Klaus Müllen,* and Akimitsu Narita*

CHEMISTRY
AN ASIAN JOURNAL

www.chemasianj.org

Accepted Article

Title: Regioselective Bromination and Functionalization of Dibenzo[hi,st]ovalene as Highly Luminescent Nanographene with Zigzag Edges

Authors: Qiang Chen, Di Wang, Martin Baumgarten, Dieter Schollmeyer, Klaus Müllen, and Akimitsu Narita

To be cited as: *Chem. Asian J.* 10.1002/asia.201801822

Link to VoR: http://dx.doi.org/10.1002/asia.201801822

A Journal of

ACES Asian Chemical Editorial Society

A sister journal of **Angewandte Chemie** and **Chemistry – A European Journal**

WILEY-VCH

10.1002/asia.201801822

WILEY-VCH

Regioselective Bromination and Functionalization of Dibenzo[*hi*,*st*]ovalene as Highly Luminescent Nanographene with Zigzag Edges

Qiang Chen,[a] Di Wang,[a] Martin Baumgarten,[a] Dieter Schollmeyer,[b] Klaus Müllen,*[a,c] and Akimitsu Narita*[a,d]

Abstract: Dibenzo[*hi*,*st*]ovalene (DBOV) is a nanographene with a combination of zigzag and armchair edges, consisting of 38 sp^2 carbons. Excellent optical properties with strong red emission have been demonstrated. Here we report the regioselective bromination of DBOV bearing two mesityl groups (**DBOV-Mes**) by treatment with *N*-bromosuccinimide (NBS) under a mild condition. The dibrominated DBOV was further subjected to transition-metal-catalyzed cross-coupling reactions, i.e. Suzuki and Sonogashira coupling, demonstrating the edge-decoration of DBOV with different functional groups. Notably, DBOVs arylated at the bay regions showed intense red emission and enhanced fluorescence quantum yields of up to 0.97. Amphoteric reduction and oxidation behavior was observed by cyclic voltammetry (CV) measurements. Chemical oxidation to stable radical cation species was also demonstrated, followed by reduction back to their neutral species.

Nanographenes, namely extended polycyclic aromatic hydrocarbons,[1] have attracted a growing interest not only because of their outstanding electronic and optical properties, but also for their wide range of potential applications in (opto-)electronic devices, such as light-emitting diodes (OLEDs) and field-effect transistors (OFETs).[2] Numerous nanographenes with armchair edge structures have been synthesized and reported, showing tunable energy gaps between the highest occupied molecular orbital (HOMO) and the lowest unoccupied molecular orbital (LUMO), mainly dependent on the shapes and sizes of their aromatic cores.[3] Edge functionalization of nanographenes has been widely studied, imparting them with intriguing properties,[4] such as n-type semiconductor characteristics,[5] intramolecular charge-transfer,[6] and/or liquid-crystalline nature,[7] distinct from their pristine, non-substituted counterparts. However, such functionalization predominantly relies on the modification of starting materials and/or precursor structures involving multiple synthetic steps, while post-synthetic direct substitution of nanographene edges has been starkly underexplored. In particular, while there are several versatile methods, such as direct borylation[8] or perchlorination of the nanographene edges,[9] selective edge-halogenation has rarely been reported,[10] despite the fact that halogen groups can be converted into various other functional groups through transition-metal-catalyzed coupling reactions.[4b, c, 5]

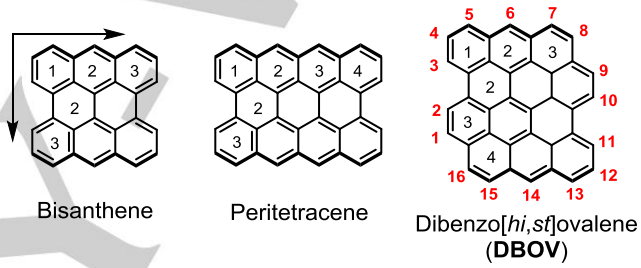

Scheme 1. Structures of representative zigzag edged nanographene molecules with different lengths and widths (from left to right: bisanthene, peritetracene and dibenzo[*hi*,*st*]ovalene (DBOV)).

Nanographenes having zigzag edges (such as anthenes and periacenes; see Scheme 1) are attracting more and more attention for their intriguing optical properties, low HOMO-LUMO gaps, and potential open-shell character.[11] However, examples of zigzag-edge nanographenes are still rather limited and the majority of them suffer from low stability, hindering further characterizations. To this end, we have recently described a synthesis of a new nanographene having zigzag edges, that is dibenzo[*hi*,*st*]ovalene (DBOV) (Scheme 1). DBOV showed sharp absorption and emission peaks in the red light region (λ_{max} = 610–625 nm) with high photoluminescence quantum yield (PLQY, Φ) up to 0.79,[12] as well as high stability under ambient conditions.[13] DBOV also exhibited amplified spontaneous emission (ASE) in a polystyrene (PS) matrix, with a low threshold of 60 μJ cm^{-2}. These characteristics make DBOV promising for light-emitting devices and bioimaging.[14] We have more recently developed an efficient synthetic route to obtain scalable amounts of DBOV derivatives using photochemical cyclization instead of the Scholl reaction.[15] However, the peripheral substitution of the DBOV core was possible only at the 6,14-positions (see Scheme 1) and at 5,13-positions through the modification of starting materials and/or reagents during the synthesis.[12-13]
In this study, we have explored the post-synthetic, direct edge-functionalization of DBOV and achieved a regioselective electrophilic bromination at 3,11-positions. The brominated DBOV could be used for transition-metal-catalyzed coupling

[a] Q. Chen, D. Wang, Prof. Dr. M. Baumgarten, Prof. Dr. K. Müllen, Dr. A. Narita
Max Planck Institute for Polymer Research
Ackermannweg 10, 55128, Mainz, Germany
E-mail: muellen@mpip-mainz.mpg; narita@mpip-mainz.mpg.de
[b] Dr. D. Schollmeyer
Institut für Organische Chemie, Johannes Gutenberg-Universität Mainz
Duesbergweg 10-14, 55099 Mainz, Germany
[c] Prof. Dr. K. Müllen
Institute of Physical Chemistry, Johannes Gutenberg-Universität Mainz
Duesbergweg 10-14, 55128 Mainz, Germany
[d] Dr. A. Narita
Organic and Carbon Nanomaterials Unit, Okinawa Institute of Science and Technology Graduate University
1919-1 Tancha, Onna-son, Kunigami, Okinawa 904-0495, Japan

Supporting information for this article is given via a link at the end of the document.((Please delete this text if not appropriate))

reactions to introduce aryl groups with electron-withdrawing substituents and triisopropylsilyl (TIPS)-protected ethynyl group. Photophysical properties and electronic structures of DBOV could be modulated by such edge-functionalization and interestingly, the obtained 3,11-aryl-substituted DBOVs demonstrated enhanced PLQY of up to 0.97.

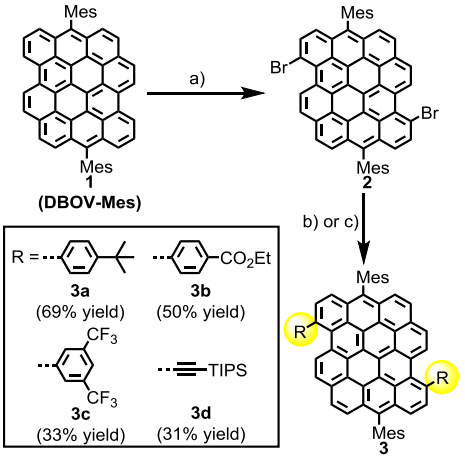

Scheme 2. Selective bromination of **DBOV-Mes** at the peripheral positions and transition-metal-catalyzed cross-coupling reactions. Conditions: a) NBS, tetrahydrofuran, r.t., 12 h, 79% yield; for **3a**–**3c**, b) $Pd(PPh_3)_4$, K_2CO_3, toluene/ethanol/water = 4:1:1, 80 °C, 12 h, 33–69% yield; for **3d**: c) $Pd(PPh_3)_4$, CuI, tetrahydrofuran/triethylamine = 1:1, 70 °C, 6 h, 31% yield.

DBOV with two mesityl groups at the 6,14-positions (**DBOV-Mes, 1**) was used to investigate the selective functionalization, considering its easy accessibility and good solubility in common solvents, such as tetrahydrofuran and toluene.[13] Mulliken charge distributions calculated using density functional theory (DFT) at the B3LYP/6-31G(d,p) level showed that the 3– and 11– positions of DBOV have higher electron density at ground state (Figure S1), which were expected to be prone to electrophilic substitution reactions. We have attempted the bromination initially by adding 2.0 equivalent of Br_2 into a solution of **DBOV-Mes** in dichloromethane, which induced a drastic change of the color from magenta to green, suggesting the oxidation of **DBOV-Mes** to cationic species. Addition of zinc powder changed the color back to magenta. Non-oxidative *N*-bromosuccinimide (NBS) was next used as bromination reagents in a mixture of chloroform and *N*,*N*-dimethylformamide, but there was no reaction even after heating at 50 °C overnight. Nevertheless, when the solvent was changed to tetrahydrofuran (THF), the bromination worked smoothly to give dibrominated product **2** (Figure S2).

The solubility of **2** was low in common organic solvents, but was sufficient for characterizations by NMR in a mixture of THF and carbon disulfide (CS_2). The ^{1}H NMR analyses revealed the disappearance of the doublet peak of **DBOV-Mes** at 9.21 ppm and exhibited 6 doublet signals after the bromination (Figure 1), indicating the selective substitution of $-H^3$ and $-H^{11}$. All protons could be assigned with the help of two-dimensional NMR techniques (Figure S11-14). High-resolution matrix-assisted laser desorption-ionization time-of-flight mass spectrometry (HR-MALDI-TOF MS) showed one intense peak located at *m/z* = 864.1015 with the isotopic distribution pattern in agreement with the calculated spectrum for $C_{56}H_{34}Br_2$ (Figure S15). Single crystals suitable for X-ray diffraction analysis were obtained by slow diffusion of acetonitrile vapor into a solution of **2** in THF/CS_2. The structure of **2** with two bromo groups at 3,11-positions (Figure 1c–d) could be unambiguously confirmed, which is in accordance with the theoretical prediction. The DBOV core appeared to be slightly distorted compared with **DBOV-Mes**. This is a result of steric repulsion between the bromo and the neighboring proton at the bay region.

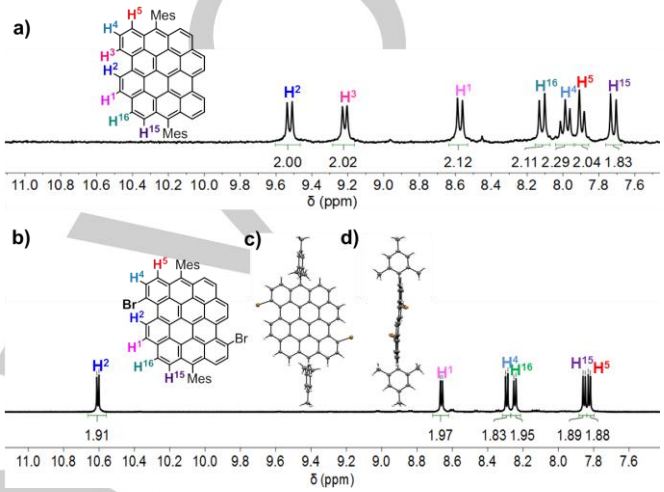

Figure 1. a) ^{1}H NMR spectra of **DBOV-Mes** in tetrahydrofuran-d_8:CS_2 = 1:1 (300 MHz, 298 K); and b) ^{1}H NMR spectra of 3,11-dibromo-6,14-dimesityldibenzo[*hi*,*st*]ovalene (**2**) in tetrahydrofuran-d_8:CS_2 = 1:1 (700 MHz, 298 K), showing the lose of $-H^3$, $-H^{11}$; c, d) X-ray single crystallographic structure of **2** (measured at 120 K): c) front view and d) side view. Hydrogens are omitted for clarity. Ellipsoids are drawn at 50% probability level.

With brominated DBOV **2** in hand, we have next investigated the possibility of further functionalization through transition-metal-catalyzed cross-coupling reactions. Suzuki coupling of **2** was carried out with substituted phenylboronic acid bearing *tert*-butyl, ethyl ester, or trifluoromethyl groups under the presence of $Pd(PPh_3)_4$ as catalyst and K_2CO_3 as base, which proceeded smoothly to provide products **3a–3c** with isolated yields ranging from 33% to 69% (Scheme 2). Sonogashira coupling of **2** was also conducted with (triisopropylsilyl)acetylene under standard conditions using $Pd(PPh_3)_4$ and CuI as catalysts and trimethylamine as base, which gave 3,11-bis(triisopropylsilyethynyl)-substituted DBOV **3d** with isolated yield of 31%. The structures of products **3a–3d** were unambiguously characterized by a combination of NMR and HR-MALDI-TOF MS analyses (see the Supporting Information).

The photophysical properties of DBOV derivatives **3a–3d** were next investigated in comparison with **DBOV-Mes** (**1**) as displayed in Figure 2. The UV-*vis*-NIR absorption and fluorescence spectra were measured in toluene solutions with a concentration of 10^{-6} M. The blue solutions of **3a–3d** showed intense absorption in the range of 500–670 nm. The absorption maxima were located at 625, 633, 630, and 646 nm, respectively, which were red-shifted by 10–35 nm in comparison with that of **DBOV-Mes**. These results indicated that the substitution of the

DBOV core with the aryl and triisopropylsilylethynyl groups slightly extended the π-conjugation. The UV-*vis*-NIR absorption of these toluene solutions did not show any changes under ambient conditions for at least 4 weeks, indicating their high stability to air and light.

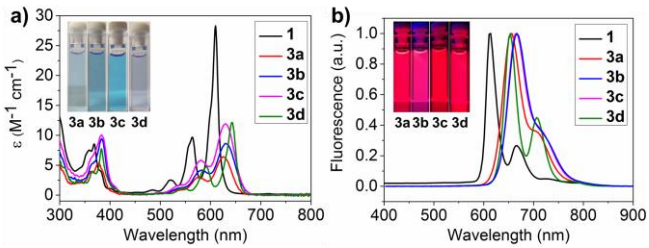

Figure 2. (a) UV-*vis*-NIR absorption and (b) fluorescence spectra of compound **1**, **3a**–**3d** in toluene with concentration of 10^{-6} M (molar absorption coefficients: **1** (2.8×10^5 $M^{-1}cm^{-1}$), **3a** (6.4×10^4 $M^{-1}cm^{-1}$), **3b** (8.5×10^4 $M^{-1}cm^{-1}$), **3c** (1.2×10^5 $M^{-1}cm^{-1}$), **3d** (1.2×10^5 $M^{-1}cm^{-1}$). Each compound was excited at their maximum absorption wavelength.

DFT (B3LYP/6-31G(d,p)) calculations were conducted to obtain better insight into the structures and electronic distributions of **3a**–**3c**. In their optimized structures, the phenyl groups are twisted by 55–57 degrees from the DBOV core (Figure S3). The relatively small dihedral angles facilitate electron conjugation between the aryl rings and the DBOV core, leading to the above-mentioned red-shifts of the absorption peaks. On the other hand, in the optimized structure of **3d**, there is obvious electron delocalization between DBOV core and the triple bonds, thus accounting for its larger red-shift of 35 nm. Additionally, time-dependent density functional theory (TDDFT) calculations at the B3LYP/6-31G(d,p) level indicated the maximum absorption wavelengths for **3a**–**3d** to be located at 649, 658, 650, and 668 nm (Table S1), respectively, which was in good agreement with the trend observed in the experimental spectra.

DBOV derivatives **3a**–**3d** showed strong fluorescence in the toluene solution with maximum emission wavelengths at 654, 667, 667, and 654 nm, respectively. The Stokes shifts are larger than that of **DBOV-Mes** because of the flexible molecule structures of **3**, where the rotation of substituted functional groups can promote the intersystem crossing. The PLQYs (Φ) of **3a**–**3d** were measured with Nile blue A perchlorate as standard by a dilution method to be 0.97, 0.94, 0.91, and 0.69, respectively.[16] It is notable that the PLQYs of aryl-substituted **3a**–**3c** were enhanced compared with **DBOV-Mes**, which might be due to the suppression of intermolecular interactions by the additional bulky substituents.

Table 1. Summary of photophysical and electrochemical data of all compounds **3a**–**3d**.

compound	λ_{abs} (nm)	Φ	E_{opt}[a] (eV)	E_{ox}^1 (V)	E_{red}^1 (V)	HOMO (eV)[b]	LUMO (eV)[b]
3a	625	0.97	1.94	0.19	-1.72	-4.91	-3.31
3b	633	0.94	1.91	0.30	-1.61	-5.04	-3.34
3c	630	0.91	1.91	0.29	-1.65	-5.02	-3.26
3d	646	0.69	1.92	0.33	-1.55	-5.05	-3.35

[a] Optical energy gap (E_{opt}) was calculated according to the crossing wavelength (λ_{cross}) of the UV-*vis*-NIR absorption and fluorescence spectra by using the following equation: $E_{opt} = 1240/\lambda_{cross}$. [b] HOMO and LUMO were calculated from the onset of their corresponding first oxidation waves and first reduction waves by using the following equation: HOMO = $-(4.8 + E_{ox}^{onset})$ eV, LUMO = $-(4.8 + E_{red}^{onset})$ eV, where E is calibrated with Fc/Fc^+.

The redox properties of DBOVs **3a**–**3d** were studied by cyclic voltammetry (CV) in THF solution using a three electrodes method with 0.1 mol/L *n*-Bu_4NPF_6 as a supporting electrolyte (Figure S4), and the electrochemical data are summarized in Table 1. The first oxidation potential of **3b** and **3c** were higher than that of **3a** as a result of the electron withdrawing groups attached to them. **3d** with triisopropylsilylethynyl groups showed the highest first oxidation potential due to more electronegative sp hybridized ethynyl carbons, which was also observed for pentacene.[17] All of these DBOVs **3a**–**3d** could be oxidized or reduced to charged species, revealing their amphoteric redox behavior.[11a, 18] The HOMO and LUMO energy levels were calculated according to the onset of the first oxidation (E_{ox}^{onset}) and reduction (E_{red}^{onset}) waves using the following equations: HOMO = $-(4.8 + E_{ox}^{onset})$ and LUMO = $-(4.8 + E_{red}^{onset})$ (see Table 1), in which the potentials were calibrated with Fc/Fc^+.

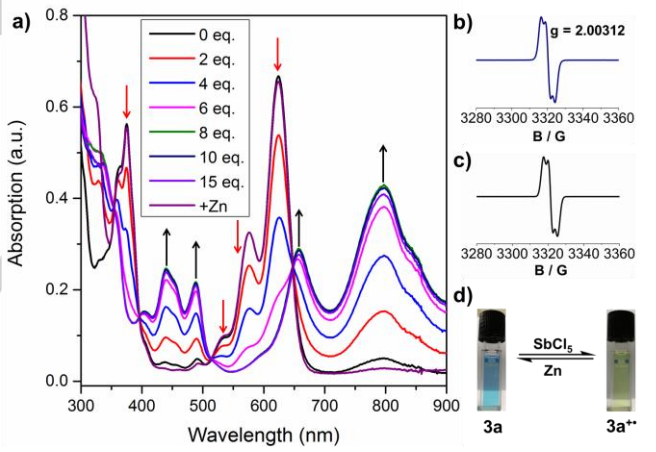

Figure 3. (a) Changes in the UV-*vis*-NIR absorption spectra during titration of **3a** with $SbCl_5$. The arrows show the changes of each peak. (b) Experimental EPR spectra after addition of 10 equivalents of $SbCl_5$ to a solution of **3a** in dry dichloromethane. (c) Simulated EPR spectra of $\mathbf{3a}^{+\bullet}$. (d) Color change of the dichloromethane solution of **3a** after oxidation with 10 equivalents of $SbCl_5$ and reduction with Zn powder.

The amphoteric redox properties of DBOV derivatives and the observation of its apparent oxidation by Br_2 prompted us to study their oxidation to radical cations. We first conducted a UV-*vis*-NIR titration of **3a**–**3d** in anhydrous dichloromethane with one electron oxidation reagent antimony chloride ($SbCl_5$). For **3a**, addition of an excess of $SbCl_5$ resulted in a continuous and gradual change of the blue solution into green with new UV-vis-NIR peaks appearing at 800, 650, 480, and 440 nm (Figure 3a). Further addition of more than 10 equivalents of $SbCl_5$ had no effect on the UV-*vis*-NIR absorption spectra, indicating the

DBOV core can only be oxidized to this state with $SbCl_5$. This phenomenon was also observed for **3b**–**3d** (Figure S7). Electron paramagnetic resonance (EPR) measurement displayed intensive signals with g factors of 2.00312 (**3a**), 2.00311 (**3b**), 2.00311 (**3c**), and 2.00330 (**3d**), indicating the formation of radical cation species (Figure S6). Interestingly, the dichloromethane solution of compound **3a** without $SbCl_5$ already contained around 12% of radical cations estimated from the UV-*vis*-NIR absorption spectra (Figure 3a), probably due to its high HOMO level, making it susceptible to oxidation by air under presence of a trace among of acid in the solvent (Table 1). It is noted that such a peak was not observed in the toluene solution of **3a** (Figure 2a). All of the oxidized species could be cleanly reduced back to the neutral state with Zn powder, indicating high stability of DBOV radical cations.

In summary, we have achieved the edge-functionalization of **DBOV-Mes** at the 3,11-positions through regioselective bromination and Suzuki or Sonogashira cross-coupling reaction. The functionalized DBOVs with aryl groups at the bay regions showed red-shifted UV-vis absorption/emission with enhanced fluorescence quantum yield and amphoteric redox properties. These results pave the way towards the synthesis of novel nanographene structures by π-extension of DBOV as well as introduction of different functional groups for further applications. For example, synthesis of water-soluble DBOV for bioimaging applications is ongoing in our laboratory.

Acknowledgements

We are grateful for the financial support from the Max Planck Society and the European Union's Horizon 2020 research and innovation programme under Marie-Curie ITN project “iSwitch” (GA No. 642196).

Keywords: Nanographene • Bromination • Post-Functionalization • Fluorescent material • Chemical oxidation

[1] a) K. Müllen and J. P. Rabe, *Acc Chem Res* **2008**, *41*, 511-520; b) J. Wu, W. Pisula and K. Müllen, *Chem. Rev.* **2007**, *107*, 718-747; c) J. Wu, A. C. Grimsdale and K. Müllen, *J. Mater. Chem.* **2005**, *15*, 41-52.

[2] a) F. Schwierz, *Nat. Nanotechnol.* **2010**, *5*, 487-496; b) K. S. Novoselov, V. I. Fal'ko, L. Colombo, P. R. Gellert, M. G. Schwab and K. Kim, *Nature* **2012**, *490*, 192-200; c) A. Narita, X. Y. Wang, X. Feng and K. Müllen, *Chem. Soc. Rev.* **2015**, *44*, 6616-6643.

[3] a) A. Stabel, P. Herwig, K. Müllen and J. P. Rabe, *Angew. Chem. Int. Ed.* **1995**, *34*, 1609-1611; b) V. S. Iyer, M. Wehmeier, J. D. Brand, M. A. Keegstra and K. Müllen, *Angew. Chem. Int. Ed.* **1997**, *36*, 1604-1607; c) V. S. Iyer, K. Yoshimura, V. Enkelmann, R. Epsch, J. P. Rabe and K. Müllen, *Angew. Chem. Int. Ed.* **1998**, *37*, 2696-2699; d) C. D. Simpson, J. D. Brand, A. J. Berresheim, L. Przybilla, H. J. Räder and K. Müllen, *Chem. Eur. J.* **2002**, *8*, 1424-1429; e) P. J. Evans, J. Ouyang, L. Favereau, J. Crassous, I. Fernandez, J. Perles and N. Martin, *Angew. Chem. Int. Ed.* **2018**, *57*, 6774-6779.

[4] a) J. Holzwarth, K. Y. Amsharov, D. I. Sharapa, D. Reger, K. Roshchyna, D. Lungerich, N. Jux, F. Hauke, T. Clark and A. Hirsch, *Angew. Chem. Int. Ed.* **2017**, *56*, 12184-12190; b) D. Joshi, M. Hauser, G. Veber, A. Berl, K. Xu and F. R. Fischer, *J. Am. Chem. Soc.* **2018**, *140*, 9574-9580; c) Y. M. Liu, H. Hou, Y. Z. Zhou, X. J. Zhao, C. Tang, Y. Z. Tan and K. Müllen, *Nat. Commun.* **2018**, *9*, 1901.

[5] A. Keerthi, B. Radha, D. Rizzo, H. Lu, V. Diez Cabanes, I. C. Hou, D. Beljonne, J. Cornil, C. Casiraghi, M. Baumgarten, K. Müllen and A. Narita, *J. Am. Chem. Soc.* **2017**, *139*, 16454-16457.

[6] A. Keerthi, I. C. Hou, T. Marszalek, W. Pisula, M. Baumgarten and A. Narita, *Chem. Asian J.* **2016**, *11*, 2710-2714.

[7] a) Y. Hu, L. F. Dössel, X.-Y. Wang, S. Mahesh, W. Pisula, S. De Feyter, X. Feng, K. Müllen and A. Narita, *ChemPlusChem* **2017**, *82*, 1030-1033; b) J. Wu, A. Fechtenkotter, J. Gauss, M. D. Watson, M. Kastler, C. Fechtenkotter, M. Wagner and K. Müllen, *J. Am. Chem. Soc.* **2004**, *126*, 11311-11321; c) J. Wu, M. D. Watson and K. Müllen, *Angew. Chem. Int. Ed.* **2003**, *115*, 5487-5491.

[8] a) H. A. Lin, Y. Sato, Y. Segawa, T. Nishihara, N. Sugimoto, L. T. Scott, T. Higashiyama and K. Itami, *Angew. Chem. Int. Ed.* **2018**, *57*, 2874-2878; b) M. N. Eliseeva and L. T. Scott, *J. Am. Chem. Soc.* **2012**, *134*, 15169-15172.

[9] Y. Z. Tan, B. Yang, K. Parvez, A. Narita, S. Osella, D. Beljonne, X. Feng and K. Müllen, *Nat. Commun.* **2013**, *4*, 2646.

[10] a) G. Li, H. Phan, T. S. Herng, T. Y. Gopalakrishna, C. Liu, W. Zeng, J. Ding and J. Wu, *Angew. Chem. Int. Ed.* **2017**, *56*, 5012-5016; b) R. Yamaguchi, S. Hiroto and H. Shinokubo, **2014**, *43*, 1637-1639.

[11] a) J. Li, K. Zhang, X. Zhang, K. W. Huang, C. Chi and J. Wu, *J. Org. Chem.* **2010**, *75*, 856-863; b) M. R. Ajayakumar, Y. Fu, J. Ma, F. Hennersdorf, H. Komber, J. J. Weigand, A. Alfonsov, A. A. Popov, R. Berger, J. Liu, K. Müllen and X. Feng, *J. Am. Chem. Soc.* **2018**, *140*, 6240-6244; c) Y. Ni, T. Y. Gopalakrishna, H. Phan, T. S. Herng, S. Wu, Y. Han, J. Ding and J. Wu, *Angew. Chem. Int. Ed.* **2018**, *57*, 9697-9701; d) Y. W. Son, M. L. Cohen and S. G. Louie, *Nature* **2006**, *444*, 347-349; e) G. Z. Magda, X. Jin, I. Hagymasi, P. Vancso, Z. Osvath, P. Nemes-Incze, C. Hwang, L. P. Biro and L. Tapaszto, *Nature* **2014**, *514*, 608-611; f) P. Ruffieux, S. Wang, B. Yang, C. Sanchez-Sanchez, J. Liu, T. Dienel, L. Talirz, P. Shinde, C. A. Pignedoli, D. Passerone, T. Dumslaff, X. Feng, K. Müllen and R. Fasel, *Nature* **2016**, *531*, 489-492.

[12] G. M. Paterno, Q. Chen, X. Y. Wang, J. Liu, S. G. Motti, A. Petrozza, X. Feng, G. Lanzani, K. Müllen, A. Narita and F. Scotognella, *Angew. Chem. Int. Ed.* **2017**, *56*, 6753-6757.

[13] D. M. Coles, Q. Chen, L. C. Flatten, J. M. Smith, K. Müllen, A. Narita and D. G. Lidzey, *Nano Lett.* **2017**, *17*, 5521-5525.

[14] a) W. Chen, S. Xu, J. J. Day, D. Wang and M. Xian, *Angew. Chem. Int. Ed.* **2017**, *56*, 16611-16615; b) L. Yuan, W. Lin, K. Zheng, L. He and W. Huang, *Chem. Soc. Rev.* **2013**, *42*, 622-661; c) C.-T. Chen, *Chem. Mater.* **2004**, *16*, 4389-4400; d) X. H. Zhang, B. J. Chen, X. Q. Lin, O. Y. Wong, C. S. Lee, H. L. Kwong, S. T. Lee and S. K. Wu, *Chem. Mater.* **2001**, *13*, 1565-1569; e) X. H. Zhu, J. Peng, Y. Cao and J. Roncali, *Chem. Soc. Rev.* **2011**, *40*, 3509-3524; f) T. Khanasa, N. Prachumrak, R. Rattanawan, S. Jungsuttiwong, T. Keawin, T. Sudyoadsuk, T. Tuntulani and V. Promarak, *Chem. Commun,* **2013**, *49*, 3401-3403.

[15] Q. Chen, W. Zajaczkowski, J. Seibel, S. Stöttinger, S. Thoms, T. Basché, S. Feyter, W. Pisula, K. Müllen and A. Narita, *Submitted*.

[16] R. Sens and K. H. Drexhage, *J. Lumin.* **1981**, *24-25*, 709-712.

[17] a) A. Maliakal, K. Raghavachari, H. Katz, E. Chandross and T. Siegrist, *Chem. Mater.* **2004**, *16*, 4980-4986; b) I. Kaur, W. Jia, R. P. Kopreski, S. Selvarasah, M. R. Dokmeci, C. Pramanik, N. E. McGruer and G. P. Miller, *J. Am. Chem. Soc.* **2008**, *130*, 16274-16286.

[18] a) T. Kubo, M. Sakamoto, M. Akabane, Y. Fujiwara, K. Yamamoto, M. Akita, K. Inoue, T. Takui and K. Nakasuji, *Angew. Chem. Int. Ed.* **2004**, *43*, 6474-6479; b) J. Li, C. Jiao, K. W. Huang and J. Wu, *Chemistry* **2011**, *17*, 14672-14680; c) Z. Zeng, Y. M. Sung, N. Bao, D. Tan, R. Lee, J. L. Zafra, B. S. Lee, M. Ishida, J. Ding, J. T. Lopez Navarrete, Y. Li, W. Zeng, D. Kim, K. W. Huang, R. D. Webster, J. Casado and J. Wu, *J. Am. Chem. Soc.* **2012**, *134*, 14513-14525.

10.1002/asia.201801822

WILEY-VCH

Entry for the Table of Contents (Please choose one layout)

Layout 1:

COMMUNICATION

Text for Table of Contents

((Insert TOC Graphic here))

*Author(s), Corresponding Author(s)**

Page No. – Page No.

Title

Layout 2:

COMMUNICATION

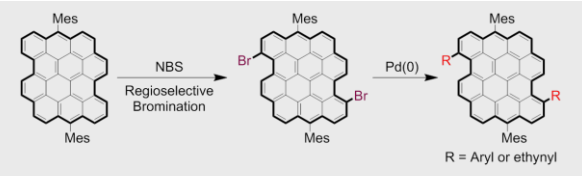

An efficient post-synthetic functionalization of dibenzo[*hi*,*st*]ovalene (DBOV) has been developed by a combination of regioselective bromination and transition-metal-catalyzed cross-coupling reactions, enabling introduction of aryl and ethynyl substituents to its 3,11-positions and demonstrating enhanced red fluorescence.

Qiang Chen, Di Wang, Martin Baumgarten, Dieter Schollmeyer, Klaus Müllen, and Akimitsu Narita**

Page No. – Page No.

Regioselective Bromination and Functionalization of Dibenzo[*hi*,*st*]ovalene as Highly Luminescent Nanographene with Zigzag Edges